Biochimica et Biophysica Acta 1812 (2011) 447–458

Contents lists available at ScienceDirect

Biochimica et Biophysica Acta

journal homepage: www.elsevier.com/locate/bbadis

Lipotoxicity and steatohepatitis in an overfed mouse model for non-alcoholic fatty liver disease

Ingrid C. Gaemers [a,*], Jan M. Stallen [a,1], Cindy Kunne [a], Christian Wallner [b], Jochem van Werven [c], Aart Nederveen [c], Wouter H. Lamers [a]

[a] University of Amsterdam, Academic Medical Center, Tytgat Institute for Liver and Intestinal Research, Meibergdreef 71, 1105 BK Amsterdam, The Netherlands
[b] University of Amsterdam, Academic Medical Center, Anatomy, Embryology & Physiology, Meibergdreef 9, 1105 AZ Amsterdam, The Netherlands
[c] University of Amsterdam, Academic Medical Center, Radiology, Meibergdreef 9, 1105 AZ Amsterdam, The Netherlands

ARTICLE INFO

Article history:
Received 11 August 2010
Received in revised form 13 December 2010
Accepted 3 January 2011
Available online 7 January 2011

Keywords:
Non-alcoholic fatty liver disease
Steatohepatitis
Liver
Overnutrition
High-fat diet
Endoplasmatic reticulum stress
Adipose tissue

ABSTRACT

The major risk factors for non-alcoholic fatty liver disease (NAFLD) are obesity, insulin resistance and dyslipidemia. The cause for progression from the steatosis stage to the inflammatory condition (non-alcoholic steatohepatitis (NASH)) remains elusive at present. Aim of this study was to test whether the different stages of NAFLD as well as the associated metabolic abnormalities can be recreated in time in an overfed mouse model and study the mechanisms underlying the transition from steatosis to NASH.
Male C57Bl/6J mice were subjected to continuous intragastric overfeeding with a high-fat liquid diet (HFLD) for different time periods. Mice fed a solid high-fat diet (HFD) *ad libitum* served as controls. Liver histology and metabolic characteristics of liver, white adipose tisue (WAT) and plasma were studied.
Both HFD-fed and HFLD-overfed mice initially developed liver steatosis, but only the latter progressed in time to NASH. NASH coincided with obesity, hyperinsulinemia, loss of liver glycogen and hepatic endoplasmatic reticulum stress. Peroxisome proliferator-activated receptor γ (*Pparγ*), fibroblast growth factor 21 (*Fgf21*), fatty acid binding protein (*Fabp*) and fatty acid translocase (CD36) were induced exclusively in the livers of the HFLD-overfed mice. Inflammation, reduced adiponectin expression and altered expression of genes that influence adipogenic capacity were only observed in WAT of HFLD-overfed mice.
In conclusion: this dietary mouse model displays the different stages and the metabolic settings often found in human NAFLD. Lipotoxicity due to compromised adipose tissue function is likely associated with the progression to NASH, but whether this is cause or consequence remains to be established.

1. Introduction

If hepatic import and synthesis of triglycerides exceeds hepatic triglyceride export and oxidation, triglycerides accumulate in the hepatocytes (steatosis stage of non-alcoholic fatty liver disease (NAFLD)). Several genetic and dietary animal models have been used to study the progression from steatosis to the stage of steatohepatitis or inflamed fatty liver (NASH; reviewed a.o. by Larter and Yeh [1]). However, the mechanisms underlying this transition have remained largely obscure due to a lack of animal models that simulate the etiology of the human disease. The severity of steatosis is significantly associated with NASH [2,3] and only part of the patients progress to steatohepatitis. Therefore it has been hypothesized that a 'double hit' is required for the development of NASH [4]: the first producing steatosis and sensitizing the liver for the second hit i.e., oxidative stress [5] or (endotoxic) cytokines [6]. However, an obligatory role for oxidative stress in the progression to NASH could not been shown [7], which led to the alternative "lipotoxicity" hypothesis (reviewed by Neuschwander-Tetri [8]). Lipotoxicity attributes cellular injury and death to fatty acids and/or their metabolites [9,10]. Although intracellular fatty acid concentration is quite constant in hepatocytes [11], the flux of fatty acids through the liver is increased in NASH patients [12,13]. This may be caused either through increased supply by excessive or inappropriate adipocyte lypolysis [14] or excessive de novo lipogenesis [15]. Combined with an imbalanced fatty acid oxidation, lipotoxicity may occur.

NAFLD is a highly prevalent disease, the worldwide incidence of which has increased significantly concomitant with the increase in the number of obese people [16]. The most common cause of obesity in man is a chronic intake of a hypercaloric diet rich in (saturated) fats. Deng et al. [17] developed a NAFLD model in which mice were continuously overfed a high-fat diet via a gastrostomy tube for 9 weeks. These mice became obese, insulin-resistant and diabetic, and developed steatohepatitis. In the present study, we used a similar mouse model in a longitudinal study to follow the development of

* Corresponding author. Tel.: +31 20 5665412; fax: +31 20 5669190.
E-mail address: i.c.gaemers@amc.uva.nl (I.C. Gaemers).
[1] Present address: Galapagos BV, Leiden, The Netherlands.

0925-4439/$ – see front matter © 2011 Elsevier B.V. All rights reserved.
doi:10.1016/j.bbadis.2011.01.003

liver pathology in time and to characterize the mechanisms underlying the progression from steatosis to NASH.

2. Materials and methods

2.1. Surgical procedure and dietary regimen

Ten-weeks old, male C57Bl/6J mice (Harlan NL) had a catheter inserted into the forestomach via a purse string suture. The catheter was attached to a 20G swivel to allow continuous infusion of feed and free movement of the mice (all infusion materials: Instech USA). From 5 post-operative days onwards, the mice were fed a, high-fat liquid diet (L10049, Research Diets, USA; Supplementary Table 1) for 3, 6 or 12 weeks (HFLD-overfed, n = 3/group). The daily amount of feed administrated increased in time from 580 kCal/kg BW (t = 0) to 750 kCal/kg BW (t = 3d), 870 kCal/kg BW (t = 7d), to the maximally tolerated amount of 920 kCal/kg BW (t = 19d; 27 kCal/day). After this, kCal/kg BW declined in time due to the maximized intake and increasing bodyweight (see Supplementary Fig. 1). A control group of 10-weeks old male C57Bl/6J mice (Harlan) without catheter had *ad libitum* access to a solid high-fat diet (D06092602, Research Diets; Supplementary Table 1) for 3, 6 or 12 weeks (HFD-fed, n = 3, 5 and 5 per group resp.). As a reference for normal values, a third group (n = 6) of male C57Bl/6J mice (Harlan NL) was included that received standard chow (Special Diets Services, #801730) and was sacrificed at the age of 17 weeks (comparable to 6 weeks fed HFD and HFLD). All mice had *ad libitum* access to water throughout the experiment. Mice were sacrificed around noon by decapitation after a brief sedation with CO_2/O_2 (70:30). Systemic blood was immediately collected into heparin-coated Pst LH microtainer tubes (BD, USA) and centrifuged. The resulting plasma was frozen in liquid N_2 and stored at −80 °C. Epididymal fat pads were removed, weighed, frozen in liquid N_2 and stored at −80 °C. The liver was removed, weighed, and parts were either fixed in 4% formaldehyde/PBS or frozen in liquid N_2 and stored at −80 °C. All experimental procedures were approved by the Institutional Animal Care and Use Committee of the Academic Medical Center.

2.2. MRI analysis of whole-body adipose tissue

After 6 weeks of diet, whole body adipose volumes were assessed (n = 3 mice/group) under ketamine-medetomidine anesthesia using a clinical 3.0 T Philips Intera MRI scanner (Philips Healthcare, Best, The Netherlands). Coronal whole body images of mice in prone position were acquired with a receive-only surface coil (5 cm diameter) using a T1-weighted Turbo Spin Echo sequence (parameters: TE/TR = 15/183 ms, NSA = 3, slice thickness 1.3 mm, no slice gap, in plain resolution 1.5 × 1.5 mm, field of view 90 × 60 mm). The signal intensity was highest at the level of the used MRI coil and lower at the cranial and caudal ends of the mice. Therefore, the signal intensity of adipose tissue along the body axis was measured in each transversal section, a conversion factor was calculated and used to normalize each section to the mid-coil section. This intensity correction was implemented in MATLAB (The MathWorks, Natick, MA, USA) and enabled computerized separation of adipose tissue from other tissues in 3D. The processed image data sets were segmented and intra-abdominal (i.e., within the peritoneal cavity) and whole-body fat volumes were determined using Amira software (Template Graphic Software, Mercury Computer Systems). To segment images, a manual threshold was set to separate the high intensity signal of adipose tissue from the lower intensity signal of non-fatty tissues and background. A lower threshold was used to separate the complete animal from the background. This way the volumes of adipose tissue and of the complete animal were determined. This was followed by manual separation of visceral and non-visceral fat in the images to determine relative visceral fat volume.

2.3. Plasma analyses

Plasma levels of alanine aminotransferase (ALAT), aspartate aminotransferase (ASAT), gamma-glutamyl transpeptidase (γ-GT), alkaline phosphatase (AP) and bilirubin were determined in a Hitachi 911 analyzer (Roche/Hitachi, Indianapolis, IN). Plasma insulin was measured with the "Ultra Sensitive Mouse Insulin ELISA" kit (Chrystal Chem Inc, USA). Plasma TNFα was measured with the "Mouse TNFα ELISA MAX" kit (BioLegend, USA). Plasma IL-6 was measured with the "BD OptEIA Mouse IL-6 ELISA" kit (BD Biosciences, USA). For detection of FABP4 protein in plasma of 6 weeks HFD-fed and HFLD-overfed mice (all n = 3/group), equal amounts of plasma were loaded on a polyacrylamidegel. Proteins were blotted on PVDF membrane and detected with a rabbit polyclonal FABP4 antibody (Cell Signaling, USA) and appropriate HRP-labeled 2nd antibody (DAKO). Chemiluminescent signals were detected using "Lumilight Plus" (Roche).

2.4. Oral glucose-tolerance test

Mice were fasted for 5 h after which blood glucose (t = 0) was measured in a drop of tail vein blood using an Elite Glucometer (Roche). In addition, a few drops of blood were collected in a heparin-coated PST LH Microtainer (BD, USA) to enable measurement of fasted insulin levels. Then mice orally received D-glucose (20% w/w solution; 1 g/kg BW). After 10, 20, 30, 60 and 90 min, blood glucose was measured in a drop of tail vein blood. The area under the curve was calculated by the trapezoidal method.

2.5. Biochemical liver analyses

Lipids were extracted from 50 to 100 mg of liver as described [18]. Triglycerides were measured using the "Trig/GB" kit (Roche). NEFA were measured using the "NEFA c" kit (WAKO, Germany). Cholesterol was measured using the "Cholesterol RTU" kit (Biomerieux, France). Phospholipids were measured using the "Phospholipids" kit (Spinreact, Spain).

2.6. Western blot analyses

50 to 100 mg of liver was homogenized in RIPA buffer (20 mM Tris (pH7.5), 150 mM NaCl, 1% NP40, 5 mM EDTA, 0.5 mM DTT, 0.2 mM PMSF) with protease and phosphatase inhibitors (both Roche). Proteins (equal μg/lane) were separated by 10% SDS-PAAGE and transferred to PVDF membrane (Millipore). Membranes were blocked in 5% BSA/TBS-T (50 mM Tris, 150 mM NaCl, 0.1% Tween-20 (pH7.5)), incubated with 1st antibody (P-Ser473-Akt, panAkt, P-Ser51-eIF2α or eIF2α (all Cell Signaling, USA)) and appropriate HRP-labeled 2nd antibody (all DAKO). Chemiluminescent signals were detected and quantified using "Lumilight Plus" (Roche) and a Lumi-Imager F1 (Roche).

2.7. (Immuno)histochemistry

Liver histology was assessed by staining formaldehyde-fixed liver sections with PicroSiriusRed (for fibrosis) and Periodic Acid Schiff (for glycogen) or by staining cryosections with Oil Red O (for steatosis). Macrophages (both infiltrating and liver-resident (Kupffer cells)) were detected in cryosections with an α-F4/80 antibody (AbD Serotec) and activated macrophages with an α-CD11b (Mac1) antibody (R&D systems). Infiltrating granulocytes and monocytes were stained with a Ly6/Gr1 antibody (BD Pharmingen).

2.8. Hepatic gene expression analyses

RNA was isolated from 50 to 100 mg frozen liver using Trizol reagent (Invitrogen, NL). cDNA was synthesized using locked oligo-dT primers (5′-TTT TTT TTT TTT TTVN-3′) and Superscript III reverse

transcriptase (Invitrogen, NL). Quantitative PCR was carried out in a Lightcycler 2.0 with the "FastStart DNA Master^{Plus} SYBR Green I" kit (Roche). Primers are shown in Supplementary Table 2. Raw Lightcycler data were analyzed using the LinReg program [19]. Measurements were corrected for between-session variation [20] and normalized for their 18S content.

2.9. Statistical analyses

Data are expressed as mean values ± SEM. All statistical tests were performed with SPSS 14.0. Data were first analyzed by two-way ANOVA to assess differences between the diet groups as a whole. Subsequently one-way ANOVA per time point and per diet was

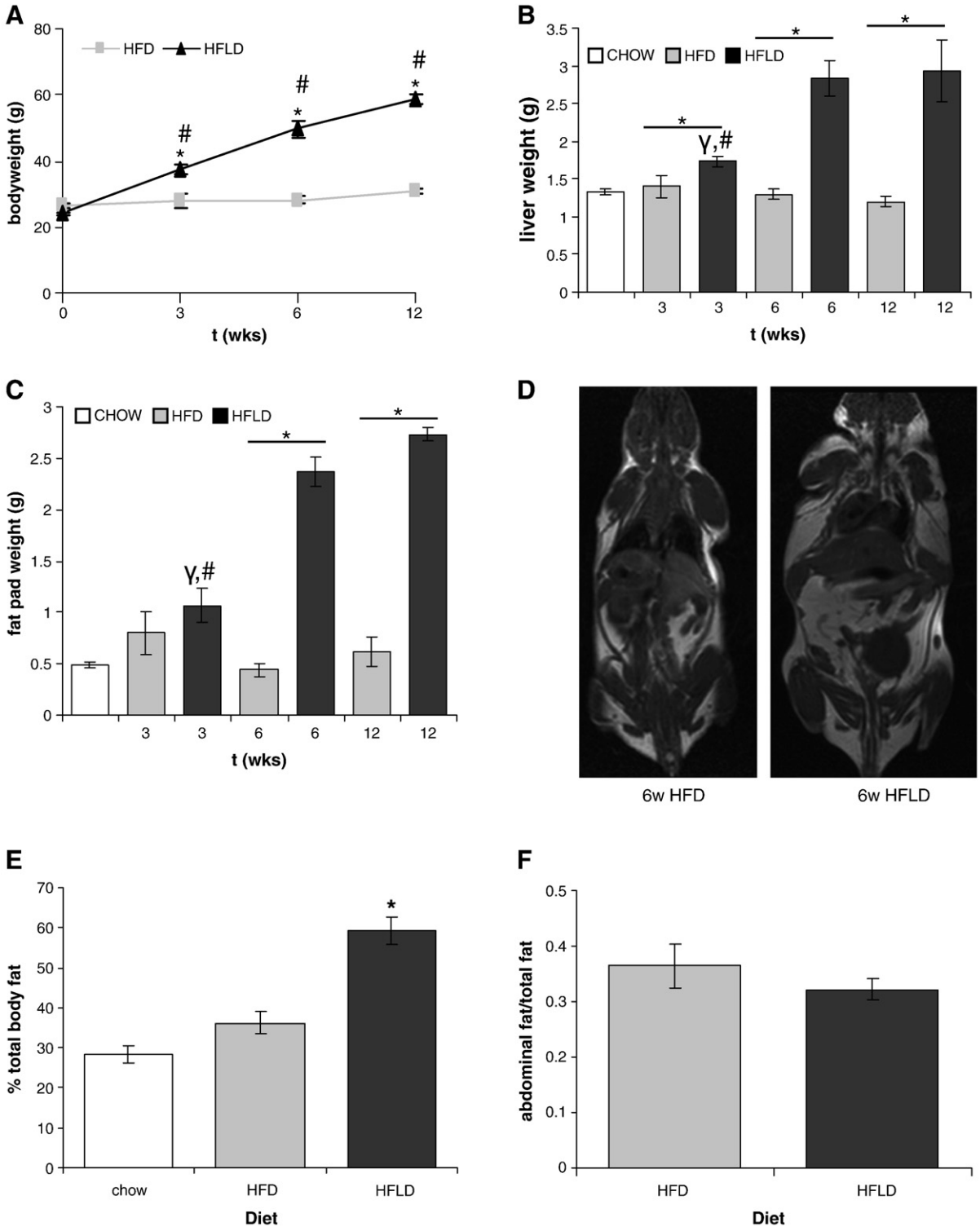

Fig. 1. Changes in bodyweight (A), liver weight (B) and fat-pad weight (C) in C57Bl6/J mice *ad libitum* fed a solid high-fat diet (HFD) or overfed a high-fat liquid diet (HFLD) for 3, 6 or 12 weeks (HFD: n = 3, 5 and 5 per group, resp. HFLD: n = 3 per group, resp.). Chow-fed mice (n = 6) were included as reference for normal values. (D) MRI quantification of total body fat in C57Bl6/J mice *ad libitum* fed a solid high-fat diet (HFD) or overfed a high-fat liquid diet (HFLD) for 6 weeks (n = 3/group). (E) Volume% total body fat as determined by MRI. (F) Ratio of intra-abdominal fat volume to total body fat volume as determined by MRI. Values represent means ± SEM. *: significantly different ($P<0.05$); #: significantly different from other groups within diet ($p<0.05$); γ: significantly different from chow ($p<0.05$).

performed, followed by Student–Newman–Keuls post hoc comparisons. $P \leq 0.05$ was considered statistically significant.

3. Results

3.1. Overfeeding a high-fat liquid diet results in a progressive increase in body, liver and fat-pad weights

Feeding C57Bl/6J male mice *ad libitum* a solid, olive-oil based, high-fat diet (HFD) resulted in a continuous and modest bodyweight gain of 20% in a period of 12 weeks (Fig. 1A). This is comparable to the normal weight gain of chow-fed C57Bl/6J male mice of similar age. In contrast, overfeeding a high-fat liquid diet (HFLD) for the same period resulted in a ~2.5-fold increase in bodyweight (Fig. 1A). The liver weights, both absolute and relative to bodyweight, were significantly increased in the HFLD-overfed mice only (Fig. 1B and Supplementary Fig. 2). The biggest effect was seen on the weight of the epididymal fat pads, especially after 6 and 12 weeks of HFLD feeding (Fig. 1C and Supplementary Fig. 2). Remarkably, the relative weights of the liver and fat pad returned to control values after 6–12 weeks of the HFD diet, whereas the effects persisted in HFLD-fed mice. Body fat volumes were also quantified using MRI imaging (Fig. 1D). The body volume and total body fat volume of the mice correlated tightly with bodyweight and epididymal fat pad weight, respectively (see Supplementary Fig. 2). The percentage total body fat almost doubled in 6 weeks HFLD-overfed mice compared to 6 weeks HFD-fed mice (Fig. 1E). Interestingly, the contribution of intra-abdominal fat to total body fat content was not different between HFD-fed and HFLD-overfed mice (Fig. 1F).

3.2. In overfed mice liver steatosis is more persistent than in HFD-fed mice

A prominent accumulation of lipid droplets was seen in the liver from the earliest time point (3 weeks) onwards in both HFD-fed and HFLD-overfed mice, but the zonal distribution of the lipid droplets was remarkably different between both high-fat fed groups (Fig. 2A and Supplementary Fig. 3). Lipid accumulated predominantly in relatively large vesicles situated around the portal veins in the HFD-fed groups. In the HFLD-overfed mice, initially a homogeneous accumulation of small lipid vesicles was observed. However, after 12 weeks of overfeeding, also large lipid droplets were present around the portal veins in addition to the homogeneously distributed smaller lipid vesicles (Fig. 2A and Supplementary Fig. 3).

Liver triglyceride levels were >10-fold higher in HFD-fed and HFLD-overfed mice than in chow-fed mice (Fig. 2B). Between 3 and 12 weeks on the high-fat diet, hepatic triglyceride content in the HFD-fed mice decreased, whereas it remained elevated in the HFLD-overfed mice (see Fig. 2B). Hepatic cholesterol, free fatty acids and phospholipids were also significantly increased in both HFD-fed and HFLD-overfed mice compared to chow-fed mice (data not shown) The persistent steatosis in the HFLD-overfed mice was also reflected by the significantly increased hepatic mRNA expression of two markers of steatotic livers: peroxisome proliferator-activated receptor γ [21,22] (*Pparγ*, Fig. 2C) and fibroblast growth factor 21 [23,24] (*Fgf21*; Fig. 2C).

Remarkably, plasma TG levels decreased ~5-fold with time in mice on the HFD diet (Fig. 2D). In mice on the HFLD diet, plasma TG levels were similar to those in chow-fed mice for the first 6 weeks on the diet, but decreased ~2-fold between 6 and 12 weeks on the diet. Plasma cholesterol levels were ~50% increased in both HFD-fed and HFLD-overfed mice from the earliest time point on the high-fat diet onwards (Fig. 2D). Plasma NEFA levels were not significantly different at any time point between any of the diets (not shown). Plasma ALAT, ASAT, AP, γ-GT or bilirubin levels were not significantly elevated in the experimental groups (data not shown).

3.3. Overfeeding causes hyperinsulinemia, but no insulin resistance

Plasma glucose levels did not differ significantly between chow-fed, HFD-fed and HFLD-overfed mice in either the fasted or the non-fasted condition (not shown). In contrast, fasted insulin levels and insulin resistance, as defined by an Oral Glucose Tolerance Test (OGTT), were slightly but significantly increased in the *ad libitum* fed group compared to the chow- and overfed groups at 6 weeks of feeding (Fig. 3A and Supplementary Fig. 4A, respectively). However, non-fasted insulin levels were significantly higher in the 12 weeks overfed mice (Fig. 4B). In the livers of 6 and 12 weeks HFLD-overfed mice, normal insulin signaling was still apparent: the degree of phosphorylation of Akt/PKB was increased (Fig. 4C) and correlated positively with plasma insulin levels ($R^2 = 0.99$; Supplementary Fig. 4B). Phosphorylation of glycogen synthase kinase 3β (GSK3β), a target of Akt/PKB, was also observed in the livers of 6 and 12 weeks HFLD-overfed mice; this correlated with the phosphorylation of Akt/PKB (data not shown).

3.4. Increased lipogenesis and lipid uptake in livers of overfed mice

To uncover putative mechanisms involved in the observed steatosis, the expression of a number of key mediators of carbohydrate and lipid metabolism was studied. The mRNA expression of fatty acid synthase (*Fas*) and stearylCoA desaturase 1 (*Scd1*), both key factors in lipogenesis, were unchanged in HFD-fed mice but were increased in the HFLD-overfed mice (Fig. 4A). In addition, the mRNA levels of fatty acid translocase (*Fat/CD36)* and fatty acid binding protein (*Fabp*), involved in fatty acid uptake and intracellular fatty acid binding respectively, were also exclusively increased in the livers of HFLD-overfed mice (Fig. 4B). Moreover, plasma FABP4 protein levels differed substantially between HFD-fed and HFLD-overfed mice (Fig. 4C).The mRNA levels of carnitine palmitoyltransferase 1 (*Cpt1a*), acetylCoA oxidase 1 (*Acox1*) and peroxisome proliferator-activated receptor α (*Pparα*), all involved in fatty acid oxidation, were not different in time and between diets (data not shown). Similarly, the mRNA expression levels of phosphoenolpyruvate caboxykinase (*Pck*), glucokinase (*Gck*) and carbohydrate-responsive element-binding protein (*Chrebp* [25]), all involved in carbohydrate metabolism, were unchanged in all groups (data not shown).

3.5. Inflammation becomes apparent with time in HFLD-overfed mouse livers only

Hepatic inflammation was assessed by immunohistochemical staining of liver sections and measuring hepatic mRNA expression of inflammation markers. Staining for the general macrophage marker F4/80 showed that the number of macrophages did not differ appreciably between chow-fed, HFD-fed and HFLD-overfed mice (Fig. 5A). At the mRNA level, liver *F4/80* expression increased ~2-fold in HFLD-overfed mice compared to chow- and HFD-fed mice (Fig. 5B). However, the number of CD11b/Mac1-positive (activated) macrophages was significantly higher in the HFLD-overfed mice at all times and increased with time to a ~10-fold difference at 12 weeks (Fig. 5A and B). The mRNA expression of Toll-like receptor 4 (*Tlr4*), also

Fig. 2. (A) Representative Oil Red O staining of liver sections of C57Bl6/J mice chow-fed (chow, n = 6/group), *ad libitum* fed a solid high-fat diet (HFD: n = 3, 5 and 5 per group, resp.) or overfed a high-fat liquid diet (HFLD: n = 3/group, resp.) for 3, 6 or 12 weeks (magnification: 5×). (B) Liver triglycerides (TG) of these mice. (C) mRNA expression of *Pparγ* and *Fgf21* relative to 18S RNA in the livers of these mice. (D) Plasma triglycerides and cholesterol of these mice. Values represent means ± SEM. *: significantly different ($p<0.05$); #: significantly different from other groups within diet ($p<0.05$); γ: significantly different from chow ($p<0.05$); $: significantly different from all other groups ($p<0.05$).

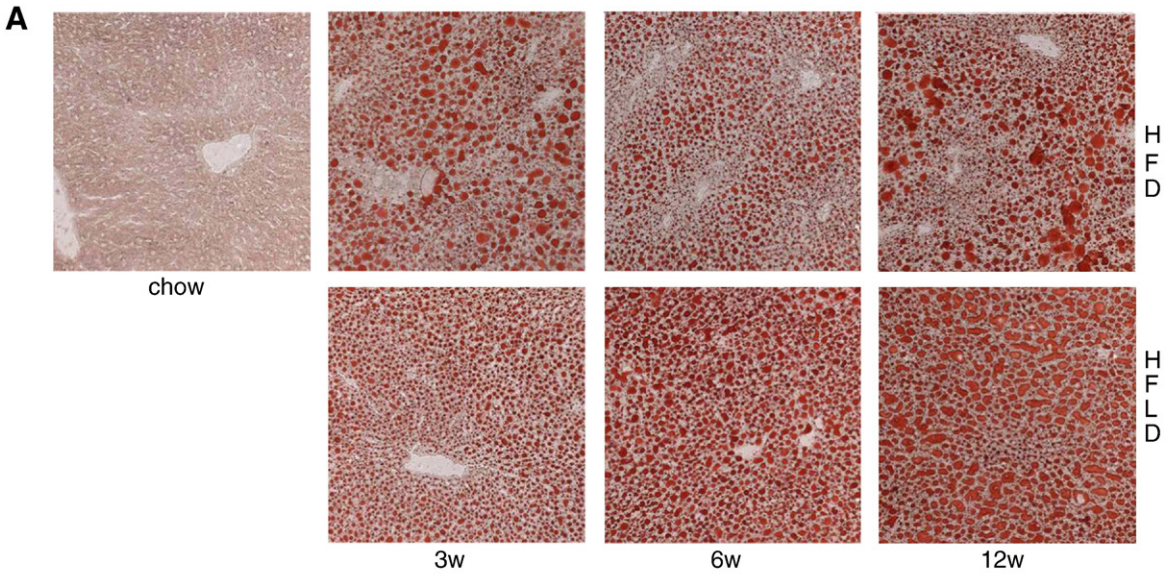
A
chow
HFD
HFLD
3w
6w
12w

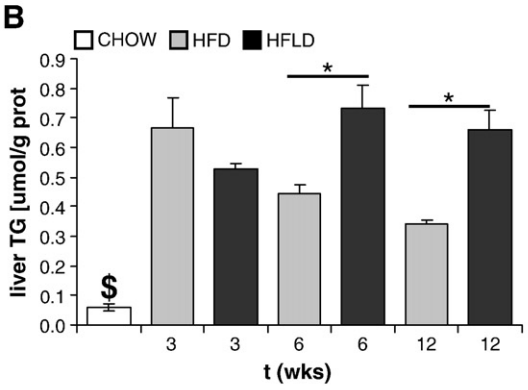
B
CHOW
HFD
HFLD
liver TG [umol/g prot
t (wks)

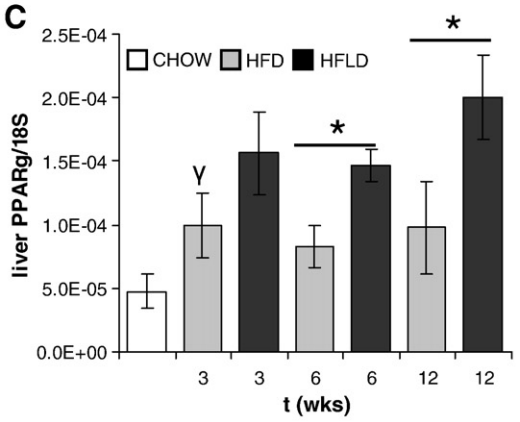
C
CHOW
HFD
HFLD
liver PPARg/18S
t (wks)

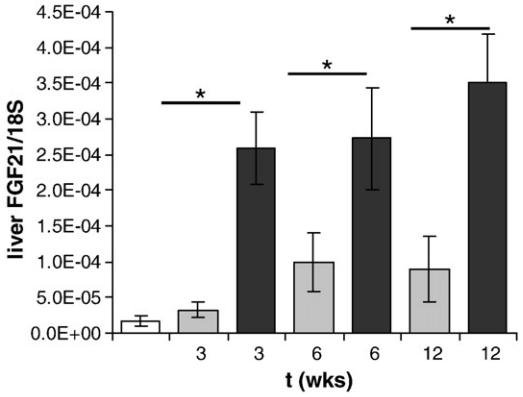
liver FGF21/18S
t (wks)

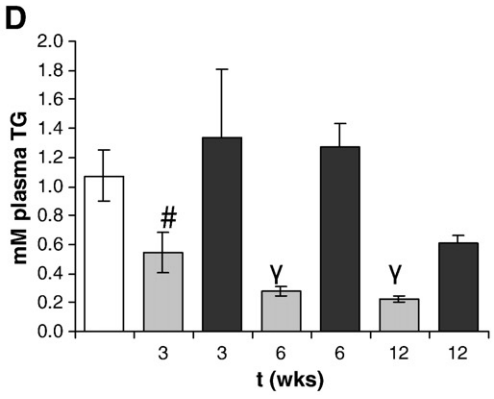
D
mM plasma TG
t (wks)

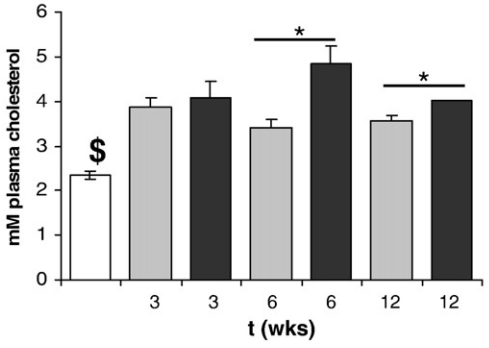
mM plasma cholesterol
t (wks)

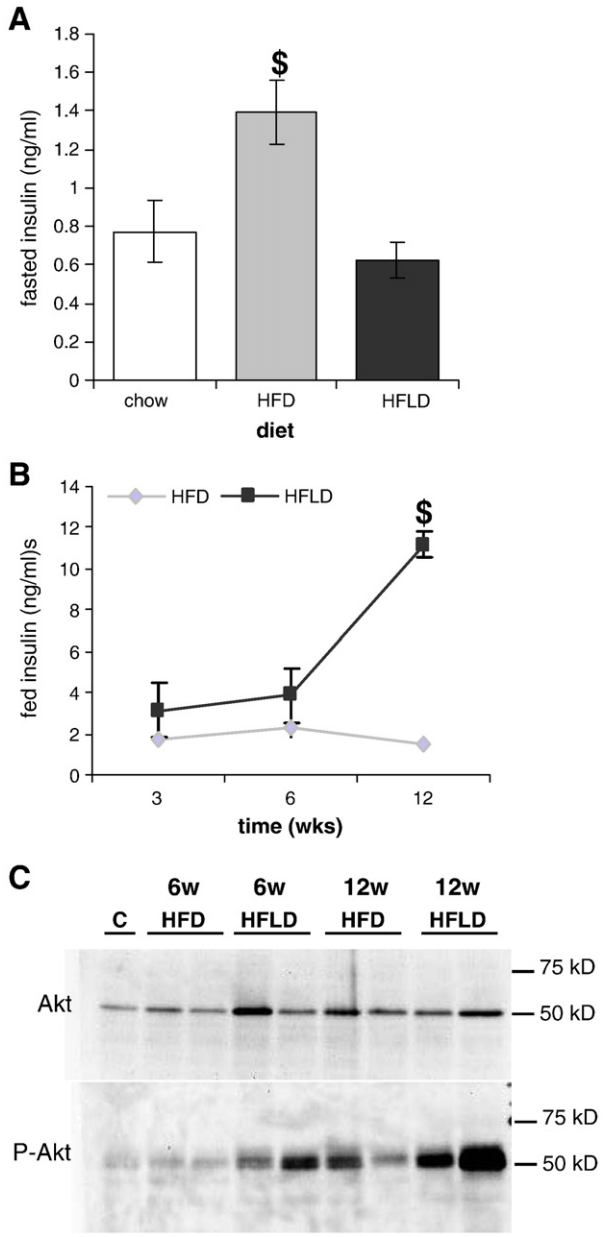

Fig. 3. (A) Plasma insulin levels of C57Bl6/J mice *ad libitum* fed a solid high-fat diet (HFD: n = 3, 5 and 5 per group, resp.) or overfed a high-fat liquid diet (HFLD: n = 3/group, resp.) for 3, 6 or 12 weeks. Values represent means ± SEM. $: significantly different from all other groups ($p<0.05$). (B) Amount of phospho-Akt/PKB (P-AKT) and total Akt on a Western blot of total protein isolated from livers of C57Bl6/J mice *ad libitum* fed a solid high-fat diet (HFD: n = 5/group, resp.) or overfed a high-fat liquid diet (HFLD: n = 3/group, resp.) for 6 or 12 weeks. Two representative samples of each group were loaded on the gel. Equal amounts of protein were loaded in each lane.

expressed on macrophages, mirrored the *CD11b*/*Mac1* data (data not shown). Most remarkable was the induction of mRNA expression of myeloperoxidase (*Mpo*) from virtually absent in chow-fed and HFD-fed mice to ~1500-fold higher levels in 12-weeks HFLD-overfed mice (Fig. 5B). *Mpo* is expressed in neutrophils and monocytes, but also in Kupffer cells [26]. The more pronounced increase in *Mpo* than in *Mac1*/*CD11b* expression implies that the increase in *Mpo* expression in the livers of HFLD-overfed mice largely reflects infiltrating neutrophils. Indeed, numerous clusters of inflammatory cells containing Ly6/Gr1-positive neutrophils or monocytes were found in the livers of HFLD-overfed mice (Fig. 5C).

None of the livers showed signs of extensive liver fibrosis except that of one 12-weeks HFLD-overfed mouse that showed extensive fibrosis (Supplementary Fig. 5). This fibrosis co-localized with large inflammatory foci. In agreement, the hepatic mRNA expression of α1procollagen (I) was not different between the different experimental groups (data not shown).

Hepatic oxidative stress and lipid peroxidation are implicated in the progression of fatty livers to NASH [27–29]. However, the fraction of oxidized glutathione (GSH/GSSG) did not differ between the experimental groups (Supplementary Fig. 6A). Furthermore, the expression of oxidative stress markers Nrf2, catalase and *Cyp2E1* was not different between HFD-fed and HFLD-overfed mice (Supplementary Fig. 6B). The expression of heme oxygenase 1 (*Ho-1*), which may respond to oxidative stress [27,30], was ~3-fold induced in the livers of HFLD-overfed mice (Fig. 6A).

Fatty-acid accumulation and exposure to cytokines both induce endoplasmatic reticulum (ER) stress, which, in turn, causes increased expression of the transcription factor C/EBP-homologous protein (*Chop*) [31]. Significantly increased levels of *Chop* mRNA were found exclusively in the livers of 12 weeks HFLD-overfed mice (Fig. 6B). In accordance, increased phosphorylation of elongation initiation factor 2α (eIF2α), the first signaling intermediate of the stress kinases [31], was found in this group only (Fig. 6C). In contrast, no differences in the splicing of *Xbp1* mRNA were observed between the respective groups, which excludes a role for the stress kinase Ire1α in the observed ER stress (data not shown).

With the exception of one (12-weeks HFD-fed) mouse, all chow and HFD-fed mice displayed a normal glycogen content (Fig. 7). In contrast, all 12-weeks HFLD-overfed mice had virtually no glycogen in their hepatocytes. The HFLD mice gradually lost their liver glycogen, because only ~one-third of the 6-weeks HFLD group had decreased amounts of glycogen in their hepatocytes. The loss of glycogen correlated with the increased expression of inflammation markers.

3.6. Overfeeding leads to inflamed adipose tissue with compromised metabolic function

Plasma tumor necrosis factor α (TNFα) levels were significantly increased at all time points in the HFLD-overfed mice only (Fig. 8A). Plasma interleukin-6 (IL6) levels also tended to be increased, though this was not statistically significant (Supplementary Fig. 7). mRNA analyses showed an approximately 20 times higher expression of both *Tnfα* and *Il6* in adipose tissue compared to liver (Fig. 8B; only WAT shown); hence the majority of the increased plasma IL-6 and TNFα levels in the overfed mice originates from adipose tissue. In addition, the mRNA expression of the general macrophage marker *F4/80* and activated macrophage marker *CD11b*/*Mac1* was also significantly increased in WAT of HFLD-overfed mice (Fig. 8C). In contrast, the mRNA expression of adiponectin, an anti-inflammatory adipokine, was significantly reduced in WAT of HFLD-overfed mice (Fig. 8D). Furthermore, the expression of vascular endothelial growth factor α (*Vegfα;* Fig. 8E), involved in vascularization and often linked to adipogenesis [32], and the expression of adipocyte differentiation markers *Pparγ* and *c*/*Ebpα*, were significantly decreased in WAT of HFLD-overfed compared to HFD-fed mice (Fig. 8F; only *c*/*Ebpα* shown). Similar results were observed for the expression of the fatty-acid transporter *CD36* and the lipid chaperone *Fabp4* (*aP2*) (Fig. 8F; only *aP2* shown).

4. Discussion

Preferably, an animal model of NAFLD should display the same liver pathology as seen in human NAFLD, i.e., steatosis, steatohepatitis and steatohepatitis plus fibrosis. In addition, this pathology should occur within the metabolic setting that is often present in human NAFLD: obesity, insulin resistance, dyslipidemia, and altered serum adipokine levels. This study used intragastric overfeeding of mice with a high-fat liquid diet [17] to induce obesity and tested whether NAFLD

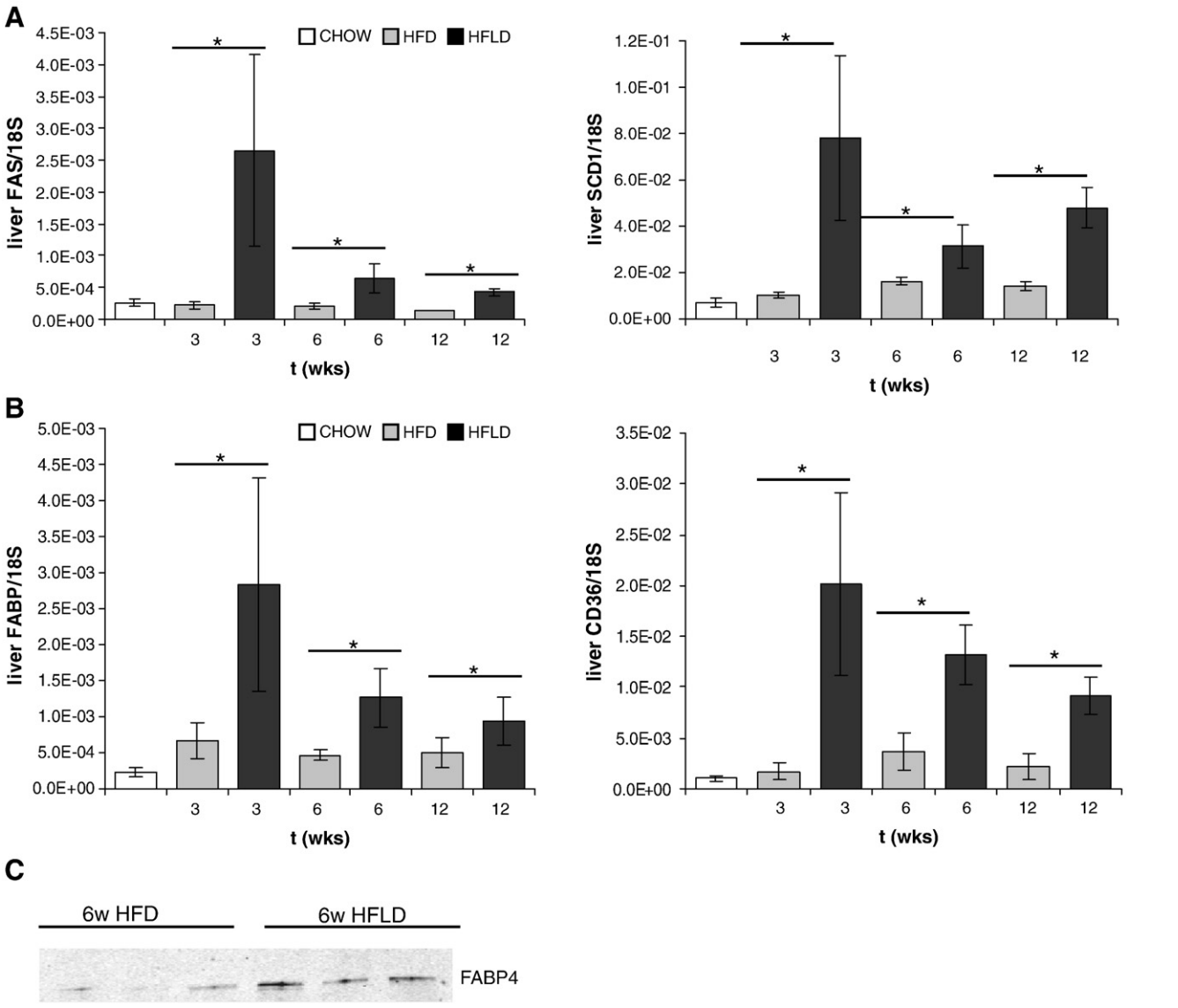

Fig. 4. mRNA expression of *Fas* and *Scd1* (A) and of *Fabp* and *Fat/Cd36* (B), relative to 18S RNA in the livers of chow-fed (n = 6), HFD-fed (n = 3, 5 and 5 per group, resp.) and HFLD-overfed mice (n = 3/group, resp.). Values represent means ± SEM. *: significantly different ($p<0.05$). C. Detection of FABP4 protein in plasma of 6 weeks HFD-fed and HFLD-overfed mice (all n = 3/group). Equal amounts of plasma were loaded in each lane.

as well as the associated metabolic abnormalities could be recreated in time. This proved to be so and as such, our data are a longitudinal extension of the data from Deng et al. [17] with a comparable but slightly less severe phenotype at the late stage of overfeeding. Although the mice in both studies are equally obese, a remarkable difference between this study and that of Deng et al. [17] is the respective absence and presence of insulin resistance. The latter may be explained by the use of different diet compositions in both studies. The lipid composition is comparable between the diets in both studies, both in terms of caloric value as well as percentage of saturated lipids. However, whereas the Deng diet uses solely (high glycemic index) glucose as carbohydrate source, (low glycemic index) maltodextrin is the main carbohydrate source in the present study. A low glycemic index diet has been shown to reduce diabetes incidence and improve diabetes control [33]. The sometimes relatively high variation in the markers we studied can be readily explained by the experience from human studies that only a fraction of patients with steatosis progress to steatohepatitis and fibrosis, and that not all patients do so at the same moment. Our rare observation of extensive fibrosis in mice corresponds with this relatively infrequent sequel of steatosis.

The livers of the overfed mice were metabolically characterized by an increased expression of (pericentrally located) lipogenic genes (*Fas, Scd1* and *Pparγ*), combined with a high portal inflow of dietary FFAs. These nutritional and metabolic sources of fat explain the observed initial homogeneous lipid accumulation in the livers of these mice. At later stages, the basal expression of lipolytic genes (*Cpt1a, Acox1* and *Pparα*), combined with the maximal inflow of dietary FFAs, cause the observed periportal lipid accumulation on top of the initially homogeneous steatosis. Unfortunately, the zonation of hepatic lipid accumulation has not been determined in other diet-induced obesity studies [17,34–37]. Carbohydrate metabolism seems to play at best a minor role in our overfed mouse model, since the expression of key factors in gluconeogenesis and glycolysis is not altered.

The mRNA expression of peroxisome proliferator-activated receptor γ (*Pparγ*) and fibroblast growth factor 21 (*Fgf21*) is significantly induced only in the livers of the HFLD-overfed mice. Previous studies have shown overexpression of both *Pparγ* and *Fgf21* in the steatotic

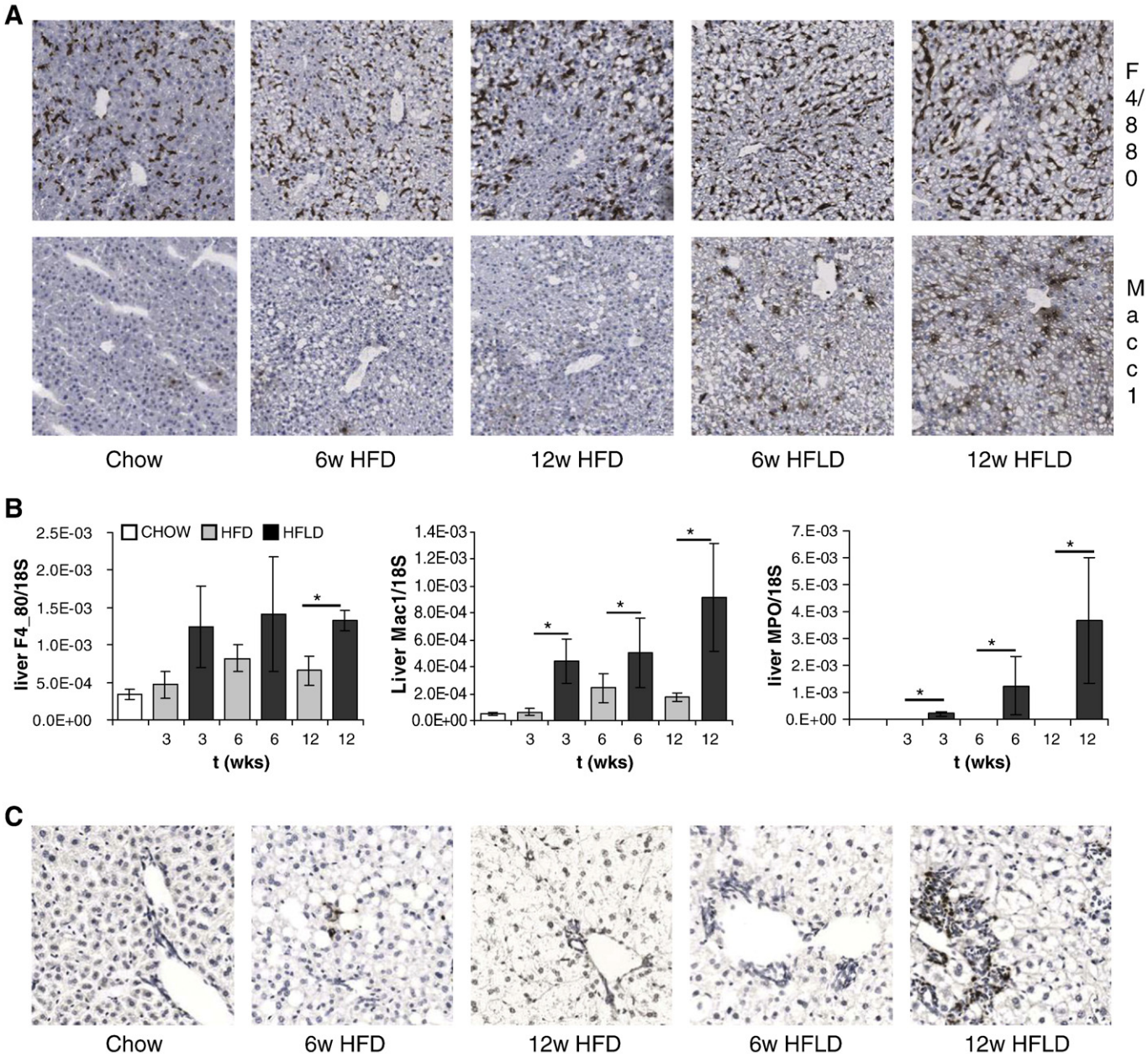

Fig. 5. (A) Liver sections of C57Bl6/J mice chow-fed (n = 6), *ad libitum* fed a solid high-fat diet (HFD: n = 5/group) or overfed a high-fat liquid diet (HFLD: n = 3/group) for 6 or 12 weeks stained for the general macrophage marker F4/80 (top row) or for Mac1/CD11b (activated macrophages). Magnification: 10×. (B) mRNA expression of *F4/80*, *Mac1/CD11b* and myeloperoxidase (*Mpo*) relative to 18S RNA in the livers of these mice. Values represent means ± SEM *: significantly different ($p<0.05$). (C) Liver sections of these mice stained for Ly6/Gr1 (granulocytes, monocytes). Magnification: 20×.

levers of obese, diabetic mice [38,39] and in liver biopsies from NAFLD patients [23,24,40]. In addition, it has been shown that PPARγ may induce FGF21 expression in mature murine 3T3L1 adipocytes [41]. Both PPARγ and FGF21 have profound effects on (lipid) metabolism, but a causal relationship between PPARγ and FGF21 in liver steatosis or steatohepatitis has not yet been established. Our data suggest such a relationship, but this requires further investigation. PPARα has also been reported to induce liver *Fgf21*, but since we find no increased expression of *Pparα* in liver of HFLD-overfed mice, PPARα is a less likely candidate for *Fgf21* induction

Hepatic steatosis *per se* is insufficient to initiate steatohepatitis, as mice *ad libitum* fed a solid high-fat diet did develop steatosis to a similar extent as mice overfed a near-identical high-fat liquid diet, but showed no increased prevalence of NASH (see also [1,36,42]). According to the "two hit" hypothesis [4,43], oxidative stress and pro-inflammatory cytokine-mediated hepatocyte injury are two putative mechanisms thought to be involved in progression to NASH. In our overfed mouse model we find no increased expression of oxidative stress markers, but we do observe increased cytokine levels.

We hypothesize that the origin for progression to NASH may very well lie within the inability of the overfed mice to adapt to the caloric overload, which leads to the severely increased adipose mass that is present in these mice. Whereas the *ad libitum* fed mice decrease their caloric intake which even results in a reduced adipose mass after 6 and 12 weeks of HFD feeding, the adipose mass in the overfed mice more than doubles from 3 to 12 weeks of overfeeding. Several studies show a relationship between adipose tisue expandibility and susceptibility to the metabolic syndrome [44–47]. Two non-exclusive models have been proposed to account for this phenomenon: In the

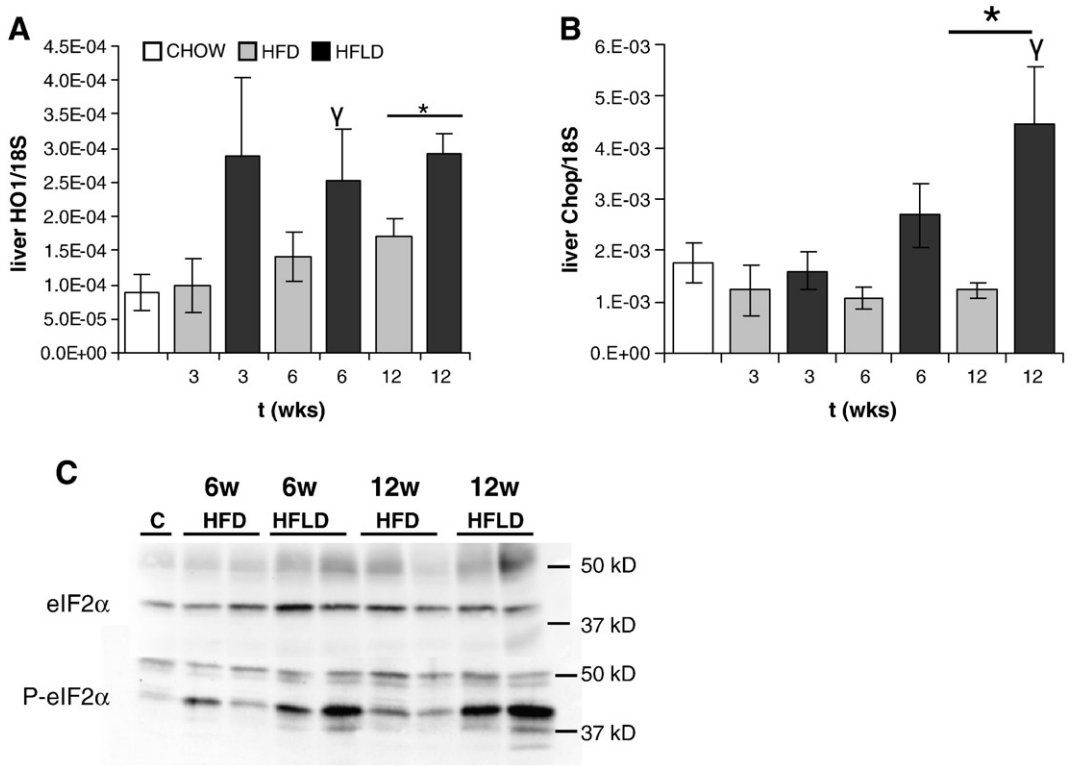

Fig. 6. mRNA expression of *Ho-1* (A) and *Chop* (B), relative to 18S RNA in the livers of chow-fed (n = 6), HFD-fed (n = 3, 5 and 5 per group, resp.) and HFLD-overfed (n = 3/group, resp.) mice. Values represent means ± SEM. *: significantly different ($p<0.05$); γ: significantly different from chow ($p<0.05$); (C) Amount of phospho-eIF2α (P-eIF2α; lower panel) and total eIF2α (top panel) on a Western blot of total protein isolated from livers of C57Bl6/J mice chow-fed (C), *ad libitum* fed a solid high-fat diet (HFD) or overfed a high-fat liquid diet (HFLD) for 6 or 12 weeks (n = 3–5 per group). Two representative samples of each group were loaded on the gel. Equal amounts of protein were loaded in each lane.

first, excessive fat accumulation is associated with chronic inflammation, increased cytokine production and altered adipokine secretion of WAT. Both cytokines and adipokines influence metabolism in peripheral tissues. In the second, lipotoxicity, model, adipocytes are metabolically changed which results in a decreased lipid storage capacity and increased lipid outflow. This causes lipotoxicity in peripheral organs. Our overfed mouse model likely displays both mechanisms since increased expression of inflammation markers and decreased expression of adiponectin, adipocyte differentiation markers *Pparγ* and *c/Ebpα* and the lipogenic genes *Fat/CD36* and *Fabp4/aP2* are observed in WAT of HFLD-overfed mice compared to WAT of HFD-fed mice. In addition, increased plasma FABP4 and increased hepatic expression of *Fat/CD36* and *Fabp* are observed in HFLD-overfed mice compared to HFD-fed mice. These observations suggest an increased flux of fatty acids through the overfed mouse livers, similar to that observed in NAFLD patients [12,13], making the lipotoxity hypothesis a likely explanation for the observed steatohepatitis in our overfed mice.

Increased visceral fat mass along with a changed serum adipokine and cytokine profile is prevalent in human NAFLD (Fan and Farrell [48] and references therein). Blood coming from visceral fat drains directly into the liver. It is therefore tempting to speculate that the increased inflow of pro-inflammatory cytokines and fatty acids and decreased inflow of anti-inflammatory adiponectin leads to the observed increase of liver macrophages and other infiltrating inflammatory cells. The above mechanisms may also account for other observed phenomena in our overfed mouse model: increased phosphorylation of eIF2α and mRNA expression of *Chop*, both markers of endoplasmatic reticulum (ER) stress, and decreased liver glycogen storage. Previous studies have shown that fatty acids and cytokines are associated with ER stress, both in rodents [49,50] and in NAFLD patients [51]. In addition, fatty acids may decrease glucose conversion into glycogen [52,53].

In conclusion, the overfed mouse model displays the characteristics of human NAFLD within the appropriate metabolic setting, i.e., obesity through overcaloric intake of a high-fat diet. It is shown that

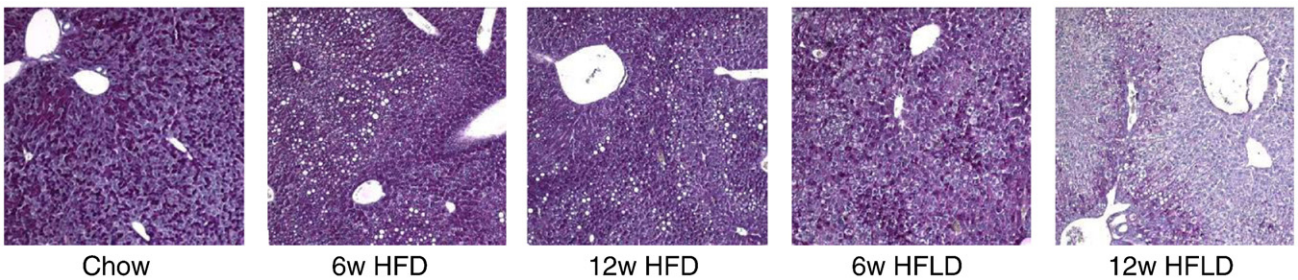

Fig. 7. Liver sections of C57Bl6/J mice chow-fed (n = 6), *ad libitum* fed a solid high-fat diet (HFD: n = 5/group, resp.) or overfed a high-fat liquid diet (HFLD: n = 3/group, resp.) for 6 or 12 weeks stained for glycogen content by Periodic acid Schiff staining. Magnification: 5×. A representative section for each group is shown.

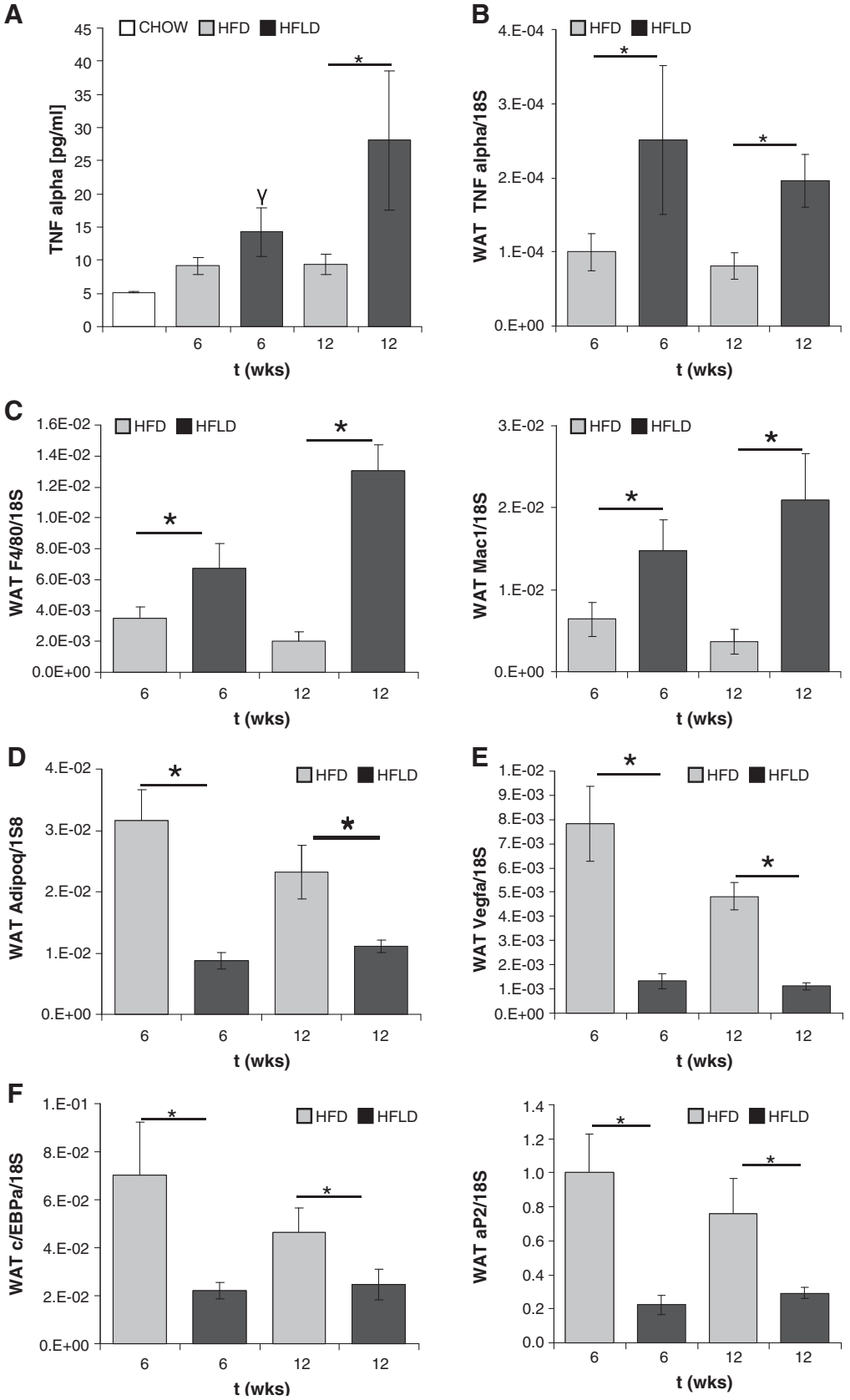

Fig. 8. (A) TNFα in plasma of C57Bl6/J mice chow-fed (chow), *ad libitum* fed a solid high-fat diet (HFD) or overfed a high-fat liquid diet (HFLD) for 6 or 12 weeks (all n = 3/group). mRNA expression of *Tnfα* (B) *F4/80* (C left panel) and *Mac1/CD11b* (C right panel), adiponectin (D), *Vegfα* (E) and *c/EBPα* (F left panel) and *aP2* (F right panel) relative to 18S RNA in WAT of these mice (all n = 3/group). Values represent means ± SEM. *: significantly different ($p<0.05$); γ: significantly different from chow ($p<0.05$).

the transition from steatosis to NASH coincides with major changes in adipose tissue. The causal relationship between NASH and the compromised function of inflamed adipose tissue requires further study.

Abbreviations

HFD High-fat diet
HFLD High-fat liquid diet

Supplementary materials related to this article can be found online at doi:10.1016/j.bbadis.2011.01.003.

Acknowledgements

Authors thank Jan M. Ruijter (statistical and MRI image analysis), Bouke A. de Boer (MRI image analysis), Nanda van Eeken (surgery) and all personnel of the AMC animal facility (ARIA). This work was supported in part by Norgine Ltd. (Uxbridge, Middlesex, UK).

References

[1] C.Z. Larter, M.M. Yeh, Animal models of NASH: getting both pathology and metabolic context right, J. Gastroenterol. Hepatol. 23 (2008) 1635–1648.
[2] I.R. Wanless, J.S. Lentz, Fatty liver hepatitis (steatohepatitis) and obesity: an autopsy study with analysis of risk factors, Hepatology 12 (1990) 1106–1110.
[3] D.E. Kleiner, E.M. Brunt, N.M. Van, C. Behling, M.J. Contos, O.W. Cummings, L.D. Ferrell, Y.C. Liu, M.S. Torbenson, A. Unalp-Arida, M. Yeh, A.J. McCullough, A.J. Sanyal, Design and validation of a histological scoring system for nonalcoholic fatty liver disease, Hepatology 41 (2005) 1313–1321.
[4] C.P. Day, O.F. James, Hepatic steatosis: innocent bystander or guilty party? Hepatology 27 (1998) 1463–1466.
[5] A. Berson, B. De, V, P. Letteron, M.A. Robin, C. Moreau, K.J. El, N. Verthier, G. Feldmann, B. Fromenty, D. Pessayre, Steatohepatitis-inducing drugs cause mitochondrial dysfunction and lipid peroxidation in rat hepatocytes, Gastroenterology 114 (1998) 764–774.
[6] S.Q. Yang, H.Z. Lin, M.D. Lane, M. Clemens, A.M. Diehl, Obesity increases sensitivity to endotoxin liver injury: implications for the pathogenesis of steatohepatitis, Proc. Natl. Acad. Sci. U. S. A. 94 (1997) 2557–2562.
[7] W.K. Syn, L. Yang, D.J. Chiang, Y. Qian, Y. Jung, G. Karaca, S.S. Choi, R.P. Witek, A. Omenetti, T.A. Pereira, A.M. Diehl, Genetic differences in oxidative stress and inflammatory responses to diet-induced obesity do not alter liver fibrosis in mice, Liver Int. 29 (2009) 1262–1272.
[8] B.A. Neuschwander-Tetri, Hepatic lipotoxicity and the pathogenesis of nonalcoholic steatohepatitis: the central role of nontriglyceride fatty acid metabolites, Hepatology 52 (2010) 774–788.
[9] Y. Lee, H. Hirose, M. Ohneda, J.H. Johnson, J.D. McGarry, R.H. Unger, Beta-cell lipotoxicity in the pathogenesis of non-insulin-dependent diabetes mellitus of obese rats: impairment in adipocyte-beta-cell relationships, Proc. Natl. Acad. Sci. U. S. A. 91 (1994) 10878–10882.
[10] H. Malhi, G.J. Gores, Molecular mechanisms of lipotoxicity in nonalcoholic fatty liver disease, Semin. Liver Dis. 28 (2008) 360–369.
[11] P. Puri, R.A. Baillie, M.M. Wiest, F. Mirshahi, J. Choudhury, O. Cheung, C. Sargeant, M.J. Contos, A.J. Sanyal, A lipidomic analysis of nonalcoholic fatty liver disease, Hepatology 46 (2007) 1081–1090.
[12] K.L. Donnelly, C.I. Smith, S.J. Schwarzenberg, J. Jessurun, M.D. Boldt, E.J. Parks, Sources of fatty acids stored in liver and secreted via lipoproteins in patients with nonalcoholic fatty liver disease, J. Clin. Invest. 115 (2005) 1343–1351.
[13] S. Nielsen, Z. Guo, C.M. Johnson, D.D. Hensrud, M.D. Jensen, Splanchnic lipolysis in human obesity, J. Clin. Invest. 113 (2004) 1582–1588.
[14] G. Musso, R. Gambino, M. Cassader, Recent insights into hepatic lipid metabolism in non-alcoholic fatty liver disease (NAFLD), Prog. Lipid Res. 48 (2009) 1–26.
[15] M.K. Pickens, J.S. Yan, R.K. Ng, H. Ogata, J.P. Grenert, C. Beysen, S.M. Turner, J.J. Maher, Dietary sucrose is essential to the development of liver injury in the methionine-choline-deficient model of steatohepatitis, J. Lipid Res. 50 (2009) 2072–2082.
[16] M. Lazo, J.M. Clark, The epidemiology of nonalcoholic fatty liver disease: a global perspective, Semin. Liver Dis. 28 (2008) 339–350.
[17] Q.G. Deng, H. She, J.H. Cheng, S.W. French, D.R. Koop, S. Xiong, H. Tsukamoto, Steatohepatitis induced by intragastric overfeeding in mice, Hepatology 42 (2005) 905–914.
[18] N.K. Srivastava, S. Pradhan, B. Mittal, R. Kumar, G.N. Gowda, An improved, single step standardized method of lipid extraction from human skeletal muscle tissue, Anal. Lett. 39 (2006) 297–315.
[19] J.M. Ruijter, C. Ramakers, W.M. Hoogaars, Y. Karlen, O. Bakker, M.J. van den Hoff, A.F. Moorman, Amplification efficiency: linking baseline and bias in the analysis of quantitative PCR data, Nucleic Acids Res. 37 (2009) e45.
[20] J.M. Ruijter, H.H. Thygesen, O.J. Schoneveld, A.T. Das, B. Berkhout, W.H. Lamers, Factor correction as a tool to eliminate between-session variation in replicate experiments: application to molecular biology and retrovirology, Retrovirology 3 (2006) 2.
[21] J.D. Browning, J.D. Horton, Molecular mediators of hepatic steatosis and liver injury, J. Clin. Invest. 114 (2004) 147–152.
[22] O. Gavrilova, M. Haluzik, K. Matsusue, J.J. Cutson, L. Johnson, K.R. Dietz, C.J. Nicol, C. Vinson, F.J. Gonzalez, M.L. Reitman, Liver peroxisome proliferator-activated receptor gamma contributes to hepatic steatosis, triglyceride clearance, and regulation of body fat mass, J. Biol. Chem. 278 (2003) 34268–34276.
[23] J. Dushay, P.C. Chui, G.S. Gopalakrishnan, M. Varela-Rey, M. Crawley, F.M. Fisher, M.K. Badman, M.L. Martinez-Chantar, E. Maratos-Flier, Increased Fibroblast Growth Factor 21 in Obesity and Nonalcoholic Fatty Liver Disease, Gastroenterology 139 (2010) 456–463.
[24] Y. Yilmaz, F. Eren, O. Yonal, R. Kurt, B. Aktas, C.A. Celikel, O. Ozdogan, N. Imeryuz, C. Kalayci, E. Avsar, Increased Serum FGF21 Levels in Patients with Nonalcoholic Fatty Liver Disease, Eur. J. Clin. Invest. 40 (2010) 887–892.
[25] K. Uyeda, J.J. Repa, Carbohydrate response element binding protein, ChREBP, a transcription factor coupling hepatic glucose utilization and lipid synthesis, Cell Metab. 4 (2006) 107–110.
[26] K.E. Brown, E.M. Brunt, J.W. Heinecke, Immunohistochemical detection of myeloperoxidase and its oxidation products in Kupffer cells of human liver, Am. J. Pathol. 159 (2001) 2081–2088.
[27] L. Malaguarnera, R. Madeddu, E. Palio, N. Arena, M. Malaguarnera, Heme oxygenase-1 levels and oxidative stress-related parameters in non-alcoholic fatty liver disease patients, J. Hepatol. 42 (2005) 585–591.
[28] N. Chalasani, J.C. Gorski, M.S. Asghar, A. Asghar, B. Foresman, S.D. Hall, D.W. Crabb, Hepatic cytochrome P450 2E1 activity in nondiabetic patients with nonalcoholic steatohepatitis, Hepatology 37 (2003) 544–550.
[29] M.D. Weltman, G.C. Farrell, P. Hall, M. Ingelman-Sundberg, C. Liddle, Hepatic cytochrome P450 2E1 is increased in patients with nonalcoholic steatohepatitis, Hepatology 27 (1998) 128–133.
[30] E.O. Farombi, Y.J. Surh, Heme oxygenase-1 as a potential therapeutic target for hepatoprotection, J. Biochem. Mol. Biol. 39 (2006) 479–491.
[31] D. Scheuner, R.J. Kaufman, The unfolded protein response: a pathway that links insulin demand with beta-cell failure and diabetes, Endocr. Rev. 29 (2008) 317–333.
[32] D. Fukumura, A. Ushiyama, D.G. Duda, L. Xu, J. Tam, V. Krishna, K. Chatterjee, I. Garkavtsev, R.K. Jain, Paracrine regulation of angiogenesis and adipocyte differentiation during in vivo adipogenesis, Circ. Res. 93 (2003) e88–e97.
[33] D.J. Jenkins, C.W. Kendall, G. Keown-Eyssen, R.G. Josse, J. Silverberg, G.L. Booth, E. Vidgen, A.R. Josse, T.H. Nguyen, S. Corrigan, M.S. Banach, S. Ares, S. Mitchell, A. Emam, L.S. Augustin, T.L. Parker, L.A. Leiter, Effect of a low-glycemic index or a high-cereal fiber diet on type 2 diabetes: a randomized trial, JAMA 300 (2008) 2742–2753.
[34] J.N. Baumgardner, K. Shankar, L. Hennings, T.M. Badger, M.J. Ronis, A new model for nonalcoholic steatohepatitis in the rat utilizing total enteral nutrition to overfeed a high-polyunsaturated fat diet, Am. J. Physiol. Gastrointest. Liver Physiol. 294 (2008) G27–G38.
[35] R. Buettner, K.G. Parhofer, M. Woenckhaus, C.E. Wrede, L.A. Kunz-Schughart, J. Scholmerich, L.C. Bollheimer, Defining high-fat-diet rat models: metabolic and molecular effects of different fat types, J. Mol. Endocrinol. 36 (2006) 485–501.
[36] M. Ito, J. Suzuki, S. Tsujioka, M. Sasaki, A. Gomori, T. Shirakura, H. Hirose, M. Ito, A. Ishihara, H. Iwaasa, A. Kanatani, Longitudinal analysis of murine steatohepatitis model induced by chronic exposure to high-fat diet, Hepatol. Res. 37 (2007) 50–57.
[37] C.S. Lieber, M.A. Leo, K.M. Mak, Y. Xu, Q. Cao, C. Ren, A. Ponomarenko, L.M. DeCarli, Model of nonalcoholic steatohepatitis, Am. J. Clin. Nutr. 79 (2004) 502–509.
[38] X. Zhang, D.C. Yeung, M. Karpisek, D. Stejskal, Z.G. Zhou, F. Liu, R.L. Wong, W.S. Chow, A.W. Tso, K.S. Lam, A. Xu, Serum FGF21 levels are increased in obesity and are independently associated with the metabolic syndrome in humans, Diabetes 57 (2008) 1246–1253.
[39] R.A. Memon, L.H. Tecott, K. Nonogaki, A. Beigneux, A.H. Moser, C. Grunfeld, K.R. Feingold, Up-regulation of peroxisome proliferator-activated receptors (PPAR-alpha) and PPAR-gamma messenger ribonucleic acid expression in the liver in murine obesity: troglitazone induces expression of PPAR-gamma-responsive adipose tissue-specific genes in the liver of obese diabetic mice, Endocrinology 141 (2000) 4021–4031.
[40] J. Westerbacka, M. Kolak, T. Kiviluoto, P. Arkkila, J. Siren, A. Hamsten, R.M. Fisher, H. Yki-Jarvinen, Genes involved in fatty acid partitioning and binding, lipolysis, monocyte/macrophage recruitment, and inflammation are overexpressed in the human fatty liver of insulin-resistant subjects, Diabetes 56 (2007) 2759–2765.
[41] H. Wang, L. Qiang, S.R. Farmer, Identification of a domain within peroxisome proliferator-activated receptor gamma regulating expression of a group of genes containing fibroblast growth factor 21 that are selectively repressed by SIRT1 in adipocytes, Mol. Cell. Biol. 28 (2008) 188–200.
[42] N. Matsuzawa, T. Takamura, S. Kurita, H. Misu, T. Ota, H. Ando, M. Yokoyama, M. Honda, Y. Zen, Y. Nakanuma, K. Miyamoto, S. Kaneko, Lipid-induced oxidative stress causes steatohepatitis in mice fed an atherogenic diet, Hepatology 46 (2007) 1392–1403.
[43] Q.M. Anstee, R.D. Goldin, Mouse models in non-alcoholic fatty liver disease and steatohepatitis research, Int. J. Exp. Pathol. 87 (2006) 1–16.
[44] J.Y. Kim, W.E. van de, M. Laplante, A. Azzara, M.E. Trujillo, S.M. Hofmann, T. Schraw, J.L. Durand, H. Li, G. Li, L.A. Jelicks, M.F. Mehler, D.Y. Hui, Y. Deshaies, G.I. Shulman, G.J. Schwartz, P.E. Scherer, Obesity-associated improvements in metabolic profile through expansion of adipose tissue, J. Clin. Invest. 117 (2007) 2621–2637.
[45] C.Z. Larter, M.M. Yeh, D.M. Van Rooyen, N.C. Teoh, J. Brooling, J.Y. Hou, J. Williams, M. Clyne, C.J. Nolan, G.C. Farrell, Roles of adipose restriction and metabolic factors

in progression of steatosis to steatohepatitis in obese, diabetic mice, J. Gastroenterol. Hepatol. 24 (2009) 1658–1668.
[46] G. Medina-Gomez, S. Gray, A. Vidal-Puig, Adipogenesis and lipotoxicity: role of peroxisome proliferator-activated receptor gamma (PPARgamma) and PPAR-gammacoactivator-1 (PGC1), Public Health Nutr. 10 (2007) 1132–1137.
[47] M.Y. Wang, P. Grayburn, S. Chen, M. Ravazzola, L. Orci, R.H. Unger, Adipogenic capacity and the susceptibility to type 2 diabetes and metabolic syndrome, Proc. Natl. Acad. Sci. U. S. A. 105 (2008) 6139–6144.
[48] J.G. Fan, G.C. Farrell, VAT fat is bad for the liver, SAT fat is not! J. Gastroenterol. Hepatol. 23 (2008) 829–832.
[49] P. Hu, Z. Han, A.D. Couvillon, R.J. Kaufman, J.H. Exton, Autocrine tumor necrosis factor alpha links endoplasmic reticulum stress to the membrane death receptor pathway through IRE1alpha-mediated NF-kappaB activation and down-regulation of TRAF2 expression, Mol. Cell. Biol. 26 (2006) 3071–3084.
[50] D. Wang, Y. Wei, M.J. Pagliassotti, Saturated fatty acids promote endoplasmic reticulum stress and liver injury in rats with hepatic steatosis, Endocrinology 147 (2006) 943–951.
[51] P. Puri, F. Mirshahi, O. Cheung, R. Natarajan, J.W. Maher, J.M. Kellum, A.J. Sanyal, Activation and dysregulation of the unfolded protein response in nonalcoholic fatty liver disease, Gastroenterology 134 (2008) 568–576.
[52] P.J. Randle, P.B. Garland, C.N. Hales, E.A. Newsholme, The glucose fatty-acid cycle. Its role in insulin sensitivity and the metabolic disturbances of diabetes mellitus, Lancet 1 (1963) 785–789.
[53] M. Manco, M. Calvani, G. Mingrone, Effects of dietary fatty acids on insulin sensitivity and secretion, Diabetes Obes. Metab. 6 (2004) 402–413.